Superconducting Properties of a Nb_3Sn Bundle Cable Made of Ultra-fine Wires

Xudong Wang, Kiyosumi Tsuchiya, Akio Terashima, Yasuo Iijima, and Akihiro Kikuchi

***Abstract*—We have been developing A15 cables made of ultra-fine wires for the high-field superconducting magnets using react-and-wind (R&W) technology. Recently, we succeeded to fabricate a bronze-processed Nb_3Sn ultra-fine wire with a minimum diameter of 30 μm. This wire contains 19 filaments and has a Cu/Non-Cu ratio of 0.89. In this study, we measured the transport critical current (I_c) of a Nb_3Sn bundle cable made by twisting 19 wires with a diameter of 50 μm at 4.2 K and under an external field up to 18 T. The Non-Cu critical current density (J_c) was also calculated from the I_c results. To replicate the R&W process, the cable was wound on glass fiber reinforced plastic cylinder (GFRP) bobbins after the heat treatment in straight geometry. To investigate the bending characteristics of the bundle cables, we prepared four GFRP bobbins with diameters of 50 mm, 30 mm, 25 mm, and 20 mm for I_c measurements. As a result, I_c degradation was observed only in the case of the 20 mm diameter bobbin. This indicates that the bending characteristics of the bundle cables are, as expected, greatly improved due to the smaller size of the wires. We also measured the critical temperature (T_c) and magnetization characteristics of the bundle cable by using a magnetic property measurement system of Quantum Design. The onset T_c was confirmed to be 17.1 K from the normalized magnetic moment. The low field Non-Cu J_c was also estimated from the magnetization data at 4.2 K, 6 K, 8 K, and 10 K.**

***Index Terms*—Nb_3Sn, ultra-fine wire, bundle cable, react-and-wind, critical current, critical temperature, magnetization.**

I. Introduction

DEVELOPMENT of high-field superconducting magnets for accelerator and nuclear fusion reactor applications using A15 superconductors is in progress [1–9]. The magnet fabrication using Nb_3Sn, a representative material for A15 superconductors, is very complicated due to the dedicated heat treatment and stress/strain sensitivity [10–13]. This problem limits the use of reacted Nb_3Sn wires and cables for coil winding. Instead of the R&W method, the wind-and-react (W&R) technology was usually adopted for the Nb_3Sn magnet fabrication. However, the W&R technique causes other issues such as dimensional changes after reaction [14, 15] and unexpected training quench [2, 5, 16]. On the other hand, the flexibility of the A15 cables could be enhanced by bundling fine wires. The flexible cable has a higher potential to overcome the limitation of the R&W technology for A15 magnets. From this point of view, we have been developing ultra-fine A15 wires to realize the magnet made by R&W technologies with the flexible cable [17–20].

Recently, we succeeded to fabricate a bronze-processed Nb_3Sn wire with a minimum diameter of 30 μm [20]. We also made several prototype bundle cables using the ultra-fine wires. In this study, we measured the transport critical current, critical temperature, and magnetization of the bundle cables made by twisting 19 wires with a diameter of 50 μm. The Non-Cu critical current density of the bundle cables was estimated from the critical current and magnetization measurements. The bending properties of the bundle cables were investigated by the R&W process.

II. Experimental Setup

The specifications of the wire and bundle cable are listed in Table 1. The bundle cable was made by twisting 19 bronze-processed Nb_3Sn wires of 50 μm diameter without soldering as shown in Fig. 1. The wire containing 19 filaments was extruded and drawn from a 45.2 mm diameter billet. The billet consists of a bronze matrix, 19 pure Nb rods inside of the matrix, a Nb barrier wrapped around the matrix, and an oxygen-free copper tube outside the matrix. Details of the strand fabrication are described in our previous studies [20].

The I_c measurements were performed at the NIMS Tsukuba Magnet Laboratory, a high magnetic field facility in Japan. To replicate the R&W process, the Nb_3Sn bundle cable was reacted in straight geometry at 650 °C for 48 hours before I_c measurements, and then wound on the GFRP bobbin and soldered to copper current leads. Four bobbins with diameters of 50 mm, 30 mm, 25 mm, and 20 mm were prepared to investigate the

TABLE I
Specifications of Nb_3Sn Wire and Bundled Cable

Parameters	Value
Nb_3Sn wire	
Outer diameter	50 μm
No. of filaments	19
Filament diameter	3 μm
Cu/Non-Cu ratio	0.89
Barrier	Nb
Bronze composition	Cu-14mass%Sn-0.3mass%Ti [20]
Nb_3Sn bundled cable	
Minimum outer diameter	250 μm
No. of strands	19
Twist pitch	4 mm

Manuscript receipt and acceptance dates will be inserted here. This work was supported by the Japan Society for the Promotion of Science KAKENHI under Grant 21H04477.

Xudong Wang, Kiyosumi Tsuchiya, and Akio Terashima are with the High Energy Accelerator Research Organization (KEK), Tsukuba 305-0801, Japan (e-mail: wanxdon@post.kek.jp).

Yasuo Iijima and Akihiro Kikuchi are with the National Institute for Materials Science (NIMS), Tsukuba, Ibaraki 305-0028, Japan.

Digital Object Identifier will be inserted here upon acceptance.

bending properties of the bundle cable as shown in Fig. 2. The bundle cable was placed in a V-shaped groove to hold it to the bobbin. Transport I_c of the bundle cable was measured by DC four probe method in liquid helium (4.2 K) and under an external magnetic field (B_{ext}) up to 18 T. The B_{ext} was applied perpendicular to the bundle cable, and the electromagnetic force induced by the B_{ext} and the transport current (I_t) on the bundle wire was directed towards the center of the bobbin. The length between I_c voltage taps of each measurement ranged from 70 mm to 140 mm, and the distance from the I_c voltage tap to the current lead was arranged longer than 30 mm to avoid heat transfer from the current lead to the I_c measurement region.

The critical temperature and magnetic moment of the Nb_3Sn bundle cable were measured by the magnetic property measurement system (MPMS) of Quantum Design. A 5-mm-long bundle cable was set in the MPMS for these measurements. The B_{ext} was applied perpendicular to the bundle cable as in the I_c measurement. For the critical temperature measurement, 1 mT was applied to the bundle cable after cooling to 4.2 K in zero field. The temperature was then swept from 4.2 K to 18 K in 0.1 K steps and from 18 K to 25 K in 0.5 K steps. The magnetic moment was measured between 5 T and –5 T after cooling to the test temperatures of 4.2 K, 6 K, 8 K, and 10 K in zero field. The B_{ext} was changed by 0.05 T steps between 1 T and –1 T, and 0.1 T steps in the higher magnetic field region.

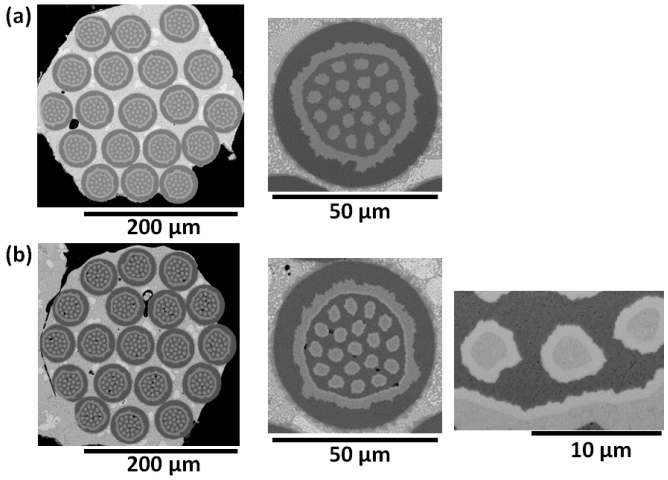

Fig. 1. Cross-sectional view of the Nb_3Sn bundled cable and wire (a) before and (b) after the heat treatment at 650 °C for 48 hours.

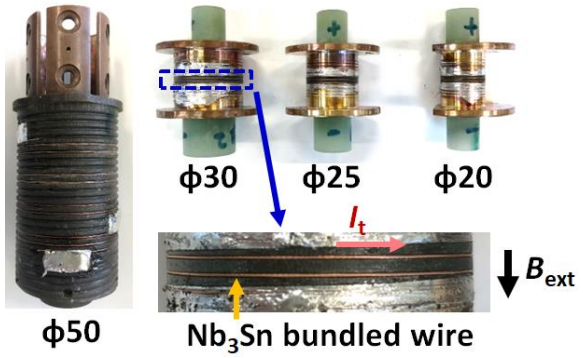

Fig. 2. Photographs of the four GFRP bobbins with diameters of 50 mm, 30 mm, 25 mm, and 20 mm. The bundled cable was wound on the bobbin and soldered to current leads after reacting.

III. Results and Discussion

A. Transport Critical Current (I_c) and Non-Cu Critical Current Density (J_c)

Fig. 3 shows the electric field versus current (*E-I*) curves measured by the four kinds of bobbins at 4.2 K and under the B_{ext} from 1 T to 18 T. The electric field was calculated by dividing the measured voltage by the distance between the I_c voltage taps for each measurement. Fig. 4 shows external magnetic field dependence on I_c and Non-Cu J_c of the four bobbin measurements and that measured without bending as a reference. The I_c was determined by 1.0 μV/cm criterion, and the Non-Cu J_c was calculated by dividing the I_c by the Non-Cu cross-sectional area (0.01974 mm^2) of the bundle cable. The reference data without bending was measured by a sample holder used in the previous study [20]. As shown in Fig. 3 and Fig. 4, I_c degradation was only observed in the bending result of the 20 mm diameter bobbin. The I_c variations between the reference data without bending and the other three bobbin measurements were within 5%. This error is mainly caused by sample-to-sample variation. The measurement error is assumed to be within 2%. In case of the no-degradation results (without bending, 50 mm,

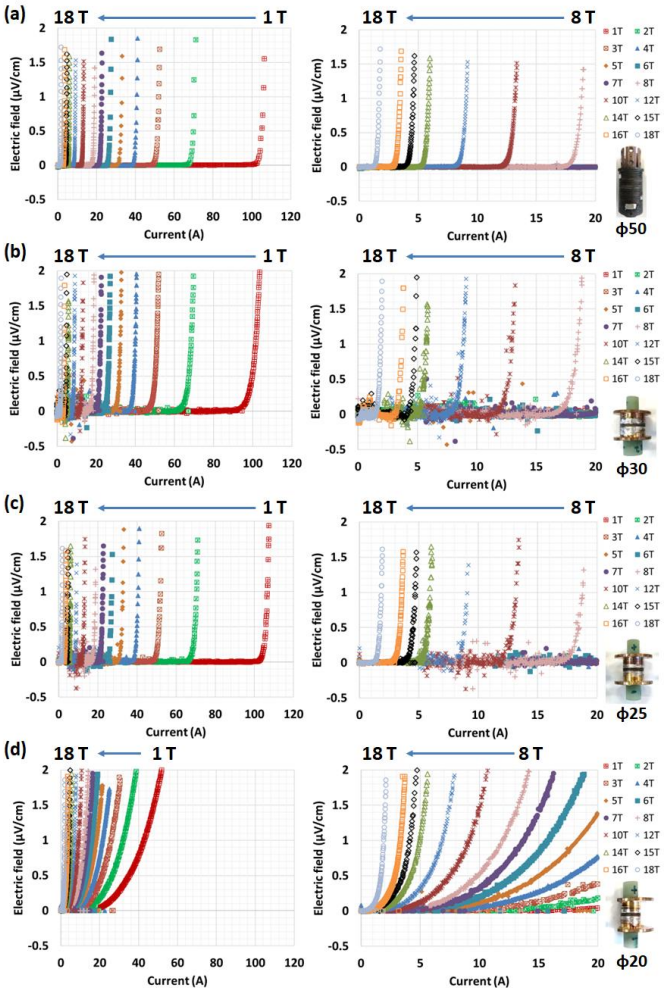

Fig. 3. *E-I* curves measured on the four bobbins with diameters of (a) 50 mm, (b) 30 mm, (c) 25 mm, and (d) 20 mm at 4.2 K and under the B_{ext} from 1 T to 18 T. Full B_{ext} results from 1 T to 18 T are shown on the left and zoomed results from 8 T to 18 T are shown on the right.

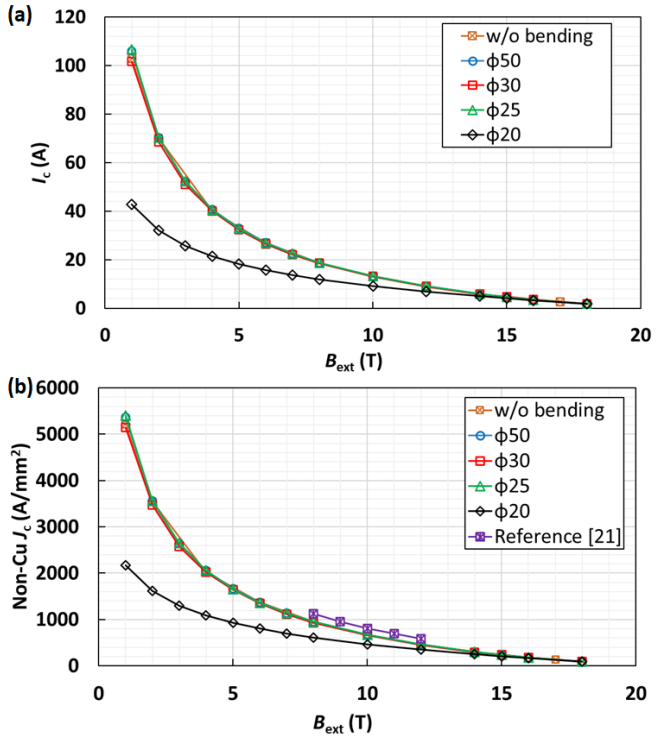

Fig. 4. Magnetic field dependance on I_c and Non-Cu J_c determined by 1.0 μV/cm. A data without bending and the four bobbin measurements with diameters of 50 mm, 30 mm, 25 mm, and 20 mm are summarized in these results. A reference data of the bronze-processed Nb_3Sn wire [21], which has 14.3%Sn almost the same as that of the test sample, is shown in Fig. 4(b).

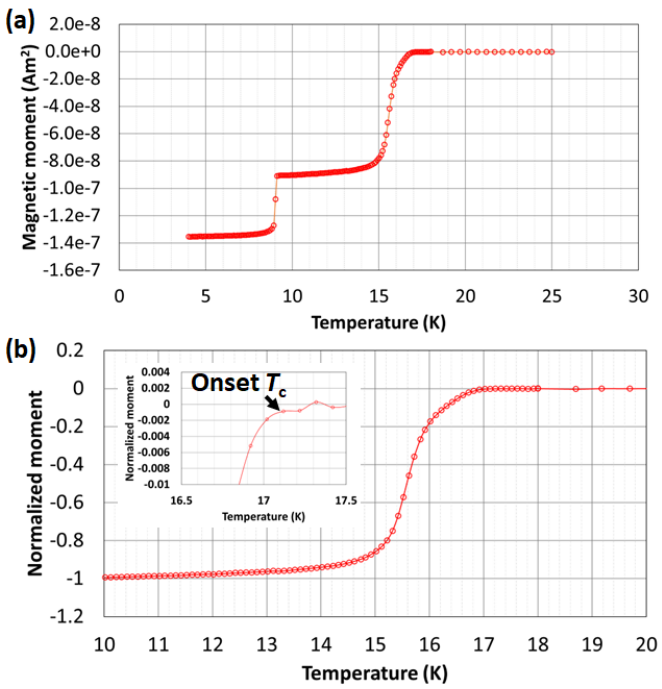

Fig. 5. Temperature dependance on (a) magnetic moment and (b) normalized moment of the Nb_3Sn bundle wire under an external magnetic field of 1.0 mT. The inset shows a magnified view around the onset T_c.

30 mm, and 25 mm), the average I_c and average Non-Cu J_c were 40 A and 2026 A/mm^2 at 4 T, 9.1 A and 461 A/mm^2 at 12 T, and 1.8 A and 91 A/mm^2 at 18 T. Comparing with the reference data [21], the Non-Cu J_c of the test sample is about 20% lower than that of the reference value. We will improve the Non-Cu J_c by increasing the Sn concentration and optimizing the bronze to Nb filament ratio in the next work.

The bending strains of the cables on the 25 mm and 20 mm bobbins are estimated to be 0.2% and 0.25% when calculated with the wire diameter of 0.05 mm. They are 1% and 1.25% when calculated with the cable diameter of 0.25 mm. Considering that the I_c degradation was not observed in the case of 25 mm bending, the 1% strain estimated from the cable diameter is too high to explain the no-degradation result compared to the previous study [10–13]. These bending properties were also observed in a thicker bundle cable made of 49 wires with the same size used in this study [20]. From these results, the bending strain of the bundle cable could be estimated to depend on the wire diameter rather than the cable diameter, and the bending limit of the cable bundling with the 50 μm wire is between 25 mm and 20 mm in diameter.

B. *Critical Temperature (T_c)*

Fig. 5 shows temperature dependance on magnetic moment and normalized moment of the bundle cable under an external magnetic field of 1 mT. Two transitions around 9 K and 17 K, which were induced by the Nb barrier and the Nb_3Sn superconductor, were observed in the measured magnetic moments. The normalized moment was determined with the average moment above 20 K as zero and the moment at 10 K as –1. The onset T_c of 17.1 K was defined by a threshold of –0.001 from the normalized moment. This T_c value agrees well with the previous study measured by DC four probe method [20].

C. *Magnetization*

Fig. 6 shows magnetization results of the bundle cable measured at 4.2 K, 6 K, 8 K, and 10 K. There is a sharp peak below 0.5 T due to the magnetization of the Nb barrier [22]. The flux jump was not observed from the sample. Fig. 7 shows the Non-Cu J_c calculated from the magnetizations at 4.2 K, 6 K, 8 K, and 10 K. These data were rescaled using the transport results for the 50 mm diameter bobbin measured at 4.2 K and 4 T as shown in Fig. 4(b). The Non-Cu J_c below 0.5 T was not shown in Fig. 7 to exclude the magnetization of the Nb barrier. The Non-Cu J_c can also be derived by (1) for the filament model using the average magnetic moment (Δm). The Δm is obtained from the measured moment in Fig. 6.

$$\text{Non-Cu } J_c = \frac{3\pi}{4}\frac{2}{d_{\text{eff}}}\frac{\Delta m}{V_{\text{Non-Cu}}} \quad (1)$$

where d_{eff} and $V_{\text{Non-Cu}}$ are the effective filament diameter of the Non-Cu area and the total Non-Cu volume of the bundle cable, respectively. The $V_{\text{Non-Cu}}$ was the product of the d_{eff} and the cable length of 5 mm. The d_{eff} of the normalized Non-Cu J_c is 15% larger than the nominal diameter in this case.

Comparing the results at 4.2 K, the error of Non-Cu J_c between the magnetization and the I_c measurement increased with

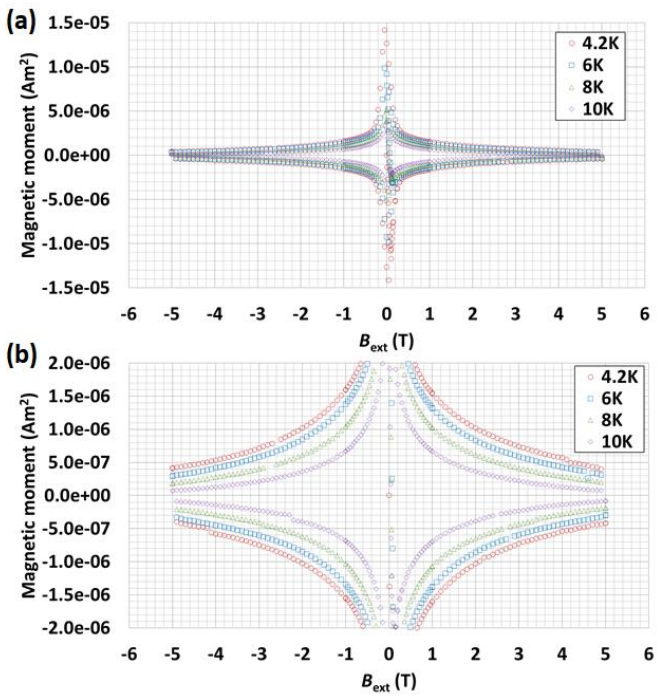

Fig. 6. Magnetization results of the Nb_3Sn bundle cable measured at 4.2 K, 6 K, 8 K, and 10 K. (a) A full-scale figure. (b) A zoomed view.

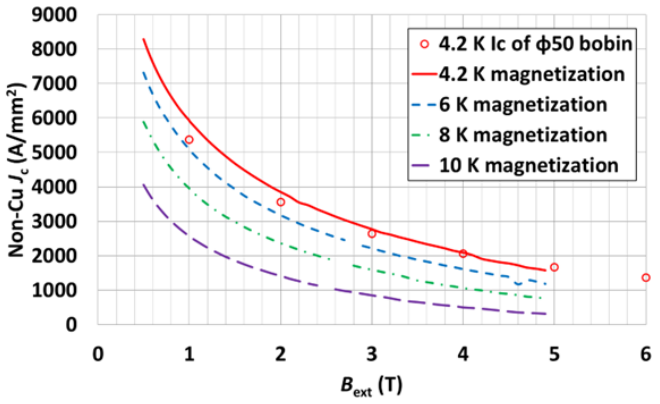

Fig. 7. Magnetic field dependance on the Non-Cu J_c obtained from the magnetizations of the Nb_3Sn bundle cable at 4.2 K, 6 K, 8 K, and 10 K. Plots are calculated from the I_c measurement at 4.2 K of the 50 mm diameter bobbin.

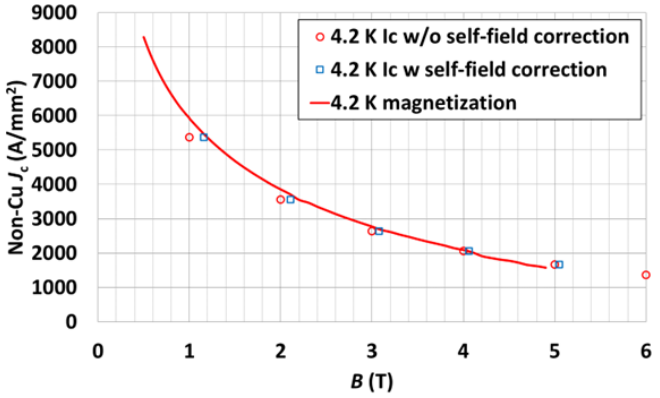

Fig. 8. Comparison of the Non-Cu J_c with and without the self-field correction at 4.2 K. Plots are calculated from the I_c measurement at 4.2 K of the 50 mm diameter bobbin, the solid line is obtained from the magnetization measured at 4.2 K.

decreasing magnetic field. This error is mainly caused by the self-field effect in the I_c measurement. The maximum self-field of the bundle cable is estimated to be about 0.0015 T/A by a 3D finite element analysis. Fig. 8 shows the comparison of the Non-Cu J_c with and without the self-field correction. The corrected Non-Cu J_c of the I_c measurement agrees well with that of the magnetization as shown in Fig. 8. The differences between the data with and without correction are 16% at 1T and less than 1.5% above 4 T. This self-field effect indicates that the fitting error between the I_c and magnetization measurements above 4 T is negligible in this case.

IV. Conclusion

We succeeded to fabricate a bronze-processed Nb_3Sn bundle cable consisting of the ultra-fine wires with a diameter of 50 µm. The magnetic field dependance on the I_c and Non-Cu J_c of the bundle cable at 4.2 K were characterized. The bundle cable was wound on the GFRP bobbin after the heat treatment in straight geometry for the measurements to replicate the R&W process. The bending properties of the bundle cable were measured by the four bobbins with diameters of 50 mm, 30 mm, 25 mm, and 20 mm. As a result, the I_c degradation was only observed from the 20 mm diameter bending. A similar result was also found in the previous study from a thicker bundle cable made of 49 wires with the same size used in this study. These experimental data indicate that the bending of the bundle cable depends on the wire size rather than the cable size, and the bending limit of the bundle cable made of the 50 µm wire is between 25 mm and 20 mm in diameter. The onset T_c of the bundle cable was 17.1 K after the reacting at 650 °C for 48 hours. The magnetizations of the bundle cable were measured at 4.2 K, 6 K, 8 K, and 10 K. The Non-Cu J_c derived from the magnetizations was compared with that of the I_c measurements. The self-field correction was sufficient to explain the error in the low field region.

References

[1] A. den Ouden, S. Wessel, E. Krooshoop, and H. ten Kate, "Application of Nb_3Sn Superconductors in High-Field Accelerator Magnets," *IEEE Trans. Appl. Supercond.*, vol. 7, no. 2, pp. 733–738, Jun. 1997.

[2] L. Chiesa, S. Caspi, M. Coccoli et al., "Performance Comparison of Nb_3Sn Magnets at LBNL," *IEEE Trans. Appl. Supercond.*, vol. 13, no. 2, pp. 1254–1257, Jun. 2003.

[3] A.V. Zlobin, G. Ambrosio, N. Andreev et al., "R&D of Nb_3Sn accelerator magnets at Fermilab," *IEEE Trans. Appl. Supercond.*, vol. 15, no. 2, pp. 1113–1118, 2005.

[4] A. Kikuchi, R. Yamada, E. Barzi et al., "Cu stabilized Nb_3Al strands for the high field accelerator magnet," *IEEE Trans. Appl. Supercond.*, vol. 18, no. 2, pp. 1026–1030, Jun. 2008.

[5] A. V. Zlobin, N. Andreev, G. Apollinari et al., "Development and test of a single-aperture 11T Nb_3Sn demonstrator dipole for LHC upgrades," *IEEE Trans. Appl. Supercond.*, vol. 23, no. 3, Jun. 2013, Art. no. 4000904.

[6] F. Savary, M. Bajko, B. Bordini et al., "Progress on the Development of the Nb_3Sn 11T Dipole for the High Luminosity Upgrade of LHC," *IEEE Trans. Appl. Supercond.*, vol. 27, no. 4, Jun. 2017, Art. no. 4003505.

[7] D. Ciazynski, "Review of Nb_3Sn conductors for ITER," *Fusion Eng. Des.*, vol. 82, pp. 488–497, 2007.

[8] N. Mitchell, D. Bessette, R. Gallix et al., "The ITER magnet system," *IEEE Trans. Appl. Supercond.*, vol. 18, no. 2, pp. 435–440, Jun. 2008.

[9] Y. Hishinuma, A. Kikuchi, Y. Iijima et al., "Study of RHQT-processed Nb_3Al multifilamentary rectangular tape strand to be applied to a fusion

magnet," *Fusion Engineering and Design*, 18, 2022, 113169.
[10] J. W. Ekin, "Strain scaling law for flux pinning in practical superconductors. Part 1: Basic relationship and application to Nb_3Sn conductors," *Cryogenics*, vol. 20, pp. 611–624, 1980.
[11] C. R. Walters, I. M. Davidson, and G. E. Tuck, "Long sample high sensitivity critical current measurements under strain," *Cryogenics*, vol. 26, pp. 406–412, 1986.
[12] W. Specking, H. Kiesel, H. Nakajima et al., "First Results of Strain Effects on I_c of Nb_3A1 Cable in Conduit Fusion Superconductors," *IEEE Trans. Appl. Supercond.*, vol. 3, no. 1, pp. 1342–1345, 1993.
[13] B. ten Haken, A. Godeke, and H. H. J. ten Kate, "The influence of compressive and tensile axial strain on the critical properties of Nb_3Sn conductors," *IEEE Trans. Appl. Supercond.*, vol. 5, pp. 1909–1912, 1995.
[14] M. Durante, L. Garcia Fajardo, P. Manil et al., "Geometrical Behavior of Nb_3Sn Rutherford Cables During Heat Treatment," *IEEE Trans. Appl. Supercond.*, vol. 26, no. 4, Jun. 2016, Art. no. 4802705.
[15] M. Michels, F. Lackner, C. Scheuerlein et al., "Length Changes of Unconfined Nb_3Sn Rutherford Cables During Reaction Heat Treatment," *IEEE Trans. Appl. Supercond.*, vol. 29, no. 5, Jun. 2019, Art. no. 6000605.
[16] G. P. Willering et al., "Cold powering tests of 11 T Nb3 Sn dipole models for LHC upgrades at CERN," *IEEE Trans. Appl. Supercond.*, vol. 26, no. 4, Jun. 2016, Art. no. 4005604.
[17] A. Kikuchi, Y. Iijima, A. Ichinose et al., "Trial manufactures of jelly-rolled Nb/Al single wire with very small diameter below 50 microns," in *Proc. IOP Conf. Ser.: Mater. Sci. Eng.*, 2020, vol. 756, Art. no. 012016.
[18] A. Kikuchi, Y. Iijima, S. Nimori et al., "Ultra-fine Nb_3Al mono-core wires and cables," *IEEE Trans. Appl. Supercond.*, vol. 31, no. 5, Aug. 2021, Art. no. 6000105.
[19] S. Kim, H. Fukuda, R. Kimura et al., "Critical Characteristics of Ultrafine Nb_3Al Superconducting Wires Under Conduction Cooling Conditions," *IEEE Trans. Appl. Supercond.*, vol. 32, no. 6, Aug. 2022, Art. no. 6001005.
[20] A. Kikuchi, Y. Iijima, M. Yamamoto, M. Kawano, and M. Otsubo, "The Bronze Processed Nb_3Sn Ultra-Thin Superconducting Wires," *IEEE Trans. Appl. Supercond.*, vol. 32, no. 4, Jun. 2022, Art. no. 6000104.
[21] G. Iwaki et al., "Development of Bronze-Processed Nb_3Sn Superconducting Wires for High Field Magnets," *IEEE Trans. Appl. Supercond.*, vol. 12, no. 1, Mar. 2002, pp. 1045–1048.
[22] D. K. Finnemore, T. F. Stromberg, and C. A. Swenson, "Superconducting properties of high-purity niobium," *Phys. Rev.*, vol. 149, pp. 231–243, 1966.